International Journal of Thermophysics, Vol. 18, No. 3, 1997

An Optical Technique for *in Situ* Density Determination in Electrolyte Solutions Under Hydrothermal Conditions

G. K. Anderson[1]

Received September 26, 1996

We report on a technique which determines the density of hydrothermal solutions through the relationship between density and refractive index given by the Lorentz Lorenz equation. An optical cell is described which allows the refractive index of fluids to be measured at temperatures up to 823 K and pressures up to 1200 bar. The validity of the Lorentz–Lorenz equation is demonstrated for pure water and water/NaCl solutions. New experimental results are presented for the density of water/$NaNO_3$ solutions at high temperature and pressure. The use of density data to derive other properties such as compressibility, thermal expansion coefficient, and apparent molar volume is demonstrated.

KEY WORDS: density; electrolyte solutions; high pressure; high temperature; hydrothermal; refractive index.

1. INTRODUCTION

Water at high temperatures and pressures has been shown to be a useful medium in which to carry out chemical reactions. Hydrothermal processing has been employed in wastewater treatment, soil remediation, organic destruction in process effluent streams, destruction of nitrates, and a host of other systems in which the chemical species of interest are in aqueous solution.

PVT information at high temperatures and pressures for multicomponent solutions is desirable for engineering purposes, as well as for modeling efforts. For dilute solutions (say, of the order of 0.1 molal ionic strength or less), the PVT properties may be usefully approximated by the properties of pure water. At higher ionic strengths. however, PVT and phase

[1] Los Alamos National Laboratory, Los Alamos, New Mexico 87545, U.S.A.

0195-928X/97/0500-0699$12.50/0

behaviors are very different from those of water. Very little has been published concerning the density of concentrated solutions at temperatures above 573 K. This paper reports on an optical technique for determining the density of solutions by measuring their refractive index. Densities for pure water and NaCl/water solutions were measured in the temperature range 473–823 K, over the pressure range 100–1000 bar. Good agreement was obtained with densities reported in the literature, measured using other techniques. New results were obtained for the densities of $NaNO_3$/water solutions over the same range of temperature and pressure. The technique measures density for many aqueous systems to an accuracy of $\pm 2\%$ and is capable of refinements that would increase the accuracy by an order of magnitude or more.

2. THEORY

The Lorentz–Lorenz equation [1, 2] gives the relationship among density, refractive index, and polarizability for a classical, one-component fluid consisting of isotropic, non-interacting molecules.

$$R \equiv \frac{1}{\rho}\frac{n^2-1}{n^2+2} = \frac{4\pi A_0 \alpha}{3M} \tag{1}$$

In the above equation, R is defined as the *specific refraction*, ρ is the mass density, n is the refractive index, A_0 is Avogadro's number, α is the molecular polarizability, and M is the molecular weight. If the wavelength of the light is far from any resonances in the molecules comprising the fluid, the polarizability (hence, refractive index) depends only weakly on the wavelength. The important point is that the polarizability is presumed to be independent of the fluid density, due to the assumption that the molecules do not interact. It is further assumed that internal degrees of freedom do not influence the polarizability; hence α is independent of temperature. Thus, under the assumptions implicit in the L-L equation, at a given wavelength, the specific refraction is a constant, and a measure of the refractive index gives the density directly, regardless of the temperature or pressure. The L-L equation may be generalized for mixtures of noninteracting molecules by the use of the molar refraction, $\tilde{R} \equiv MR$.

$$\tilde{R}_i \equiv \frac{M_i}{\rho_i}\frac{n_i^2-1}{n_i^2+2} = \frac{4\pi A_0 \alpha_i}{3} \tag{2}$$

$$\tilde{R}_{\text{mix}} = \sum_i x_i \tilde{R}_i = \frac{M_{\text{mix}}}{\rho_{\text{mix}}}\frac{n_{\text{mix}}^2-1}{n_{\text{mix}}^2+2} \tag{3}$$

Equations (2) and (3) state that if the molar refractions of the pure components of a mixture are known, then the molar refraction of the mixture may be calculated. Once $\tilde{R}_{mix}$ is known, a measurement of the refractive index can be used to determine the density, just as for single-component fluids.

Given the large number of assumptions made, it may seem surprising that the Lorentz–Lorenz equation is obeyed even approximately, for pure fluids *or* for mixtures. After all, molecules in a fluid *do* interact with each other, are in general not isotropic, and *do* have internal degrees of freedom. However, for reasons discussed below, the L-L equation is a very good approximation, even for highly associated fluids like water and for concentrated electrolyte solutions in water. That is, these fluids exhibit a specific refraction that remains nearly constant over a wide range of temperature and density. Thus, the specific refraction of a solution may be determined by measuring the refractive index and density at room temperature, after which the density may be determined at any temperature and pressure by a measurement of the refractive index.

3. EXPERIMENTAL PROCEDURE

The optical cell for observation of phase behavior and measurement of refractive index is shown in Fig. 1. It is a commercial high-pressure weld tee fitting made of Inconel 625, with dimensions $2.5 \times 3.8 \times 5.1$ cm. The tee is bored transversely and coned to accept diamond windows, which are held in place by pusher blocks which are backed by spring washers, both made from Inconel 718, an alloy which maintains its strength at high temperatures. The spring washers are necessary to maintain compression on the diamonds during temperature cycling. Gold washers, 0.0076 cm thick, are used to seal the diamonds to the cell. The inner faces (culets) of the diamonds are 1.0 mm in diameter and approximately 5.0 mm apart. The cell is surrounded by an insulated, nickel-plated brass block which is heated by four 300-W Watlow cartridge heaters. An Omega CN9000A temperature controller is used to control the temperature of the block to within 1°C. Fluids enter and exit the cell through 0.635-cm-outer diameter, high-pressure Inconel tubing. Auxiliary heaters are placed around the tubes where they enter the cell, to keep the viewed region as isothermal as possible. Since the viewed region of the cell is not isolated by hot valves, the auxiliary heaters are also required in order to minimize the tendency of cold, dense fluid in the feed tubes to mix with the hot, light fluid in the space between the windows. By keeping the region of large temperature gradients about 10 cm away from the windows, the auxiliary heaters minimize (but do not entirely eliminate) the mixing problem. The temperature

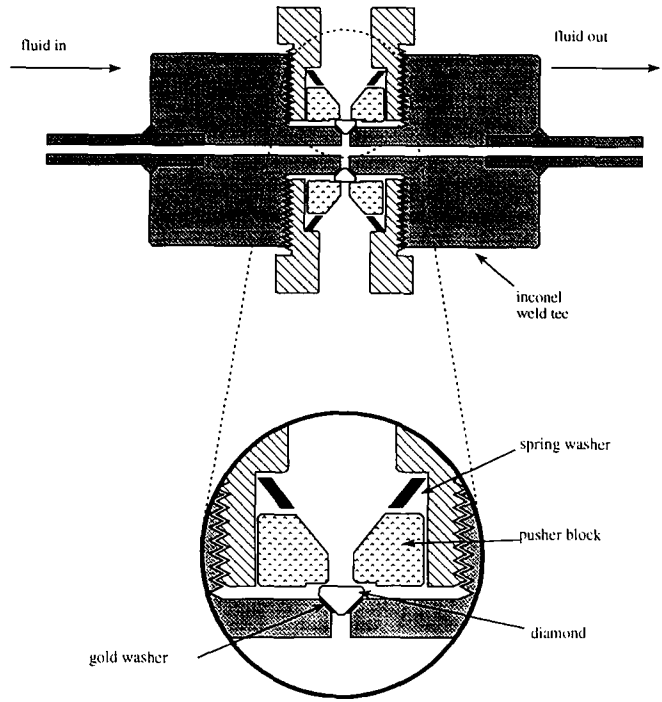

Fig. 1. Schematic of the optical cell with detail showing how diamond windows are seated. Viewed region is 1.0 mm in diameter and 5.0 mm wide.

of the fluid in the cell is measured by three sheathed, type-K thermocouples, which are inserted into the tubes which feed the cell and are read by an Omega DP-41, 10-channel readout. The ends of the thermocouple sheaths are within 1 mm of the viewed region of the cell.

Figure 2 shows a schematic of the flow system used for flushing, filling, and pressure control of the cell. High-pressure 0.635 and 0.159-cm-diameter stainless-steel. Inconel, or Hastelloy tubing is used throughout. Except as otherwise noted, all valves, tees, crosses, reducers, etc., are commercially available fittings manufactured by the High Pressure Equipment Company. The inlet to the cell is fed by a Haskel Model 300-HSF-C air-driven fluid pump, adjusted to deliver a maximum pressure of 1500 bar. The tube exiting the top of the cell goes to a valve, and thence to a waste container, and is used only for flushing and removal of trapped gases from the cell. The tube exiting the cell on the far side goes to a four-way cross. One arm of the cross goes to a Heise Model 623 pressure transducer (approximately 0–2000 bar), which is read out by a digital voltmeter. The stated accuracy

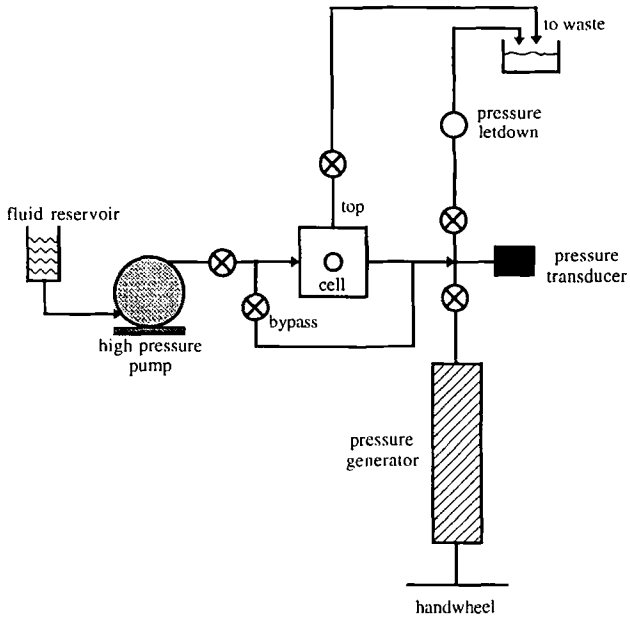

Fig. 2. Schematic of the flow system for filling, pressure control, and pressure measurement of optical cell.

of the transducer is better than 0.1%. Another arm of the cross goes to a Nupro Model R3A-H pressure letdown, adjustable between ambient pressure and 500 bar. When this arm is accessed, fluid may be pumped through the cell at constant pressure. Refractive index measurements are always made in static fluid, however. The fourth arm of the cross goes to a pressure generator (High Pressure Equipment Company, Model 37-6-30). By turning a handwheel, the pressure generator allows precise pressure adjustment in the cell. Small-diameter tubing is used to connect the various sections of the system together. This tubing was occasionally subject to plugging due to the buildup of corrosion products. Precipitation of salts is not a problem because all of the small-diameter lines are at room temperature. Plugging problems can be immediately noted and corrected by observing the system behavior. For example, if the pressure transducer does not respond to movement of the handwheel, a plug in the line to either the transducer or the pressure generator is apparent.

The optical system used for refractive index measurements is shown in Fig. 3. Light from a 100-W tungsten–halogen lamp is collimated, filtered to isolate the spectral region of the sodium-d line (589.3 nm), and focused into one of the cell windows. On the opposite side of the cell, a 5-cm-focal

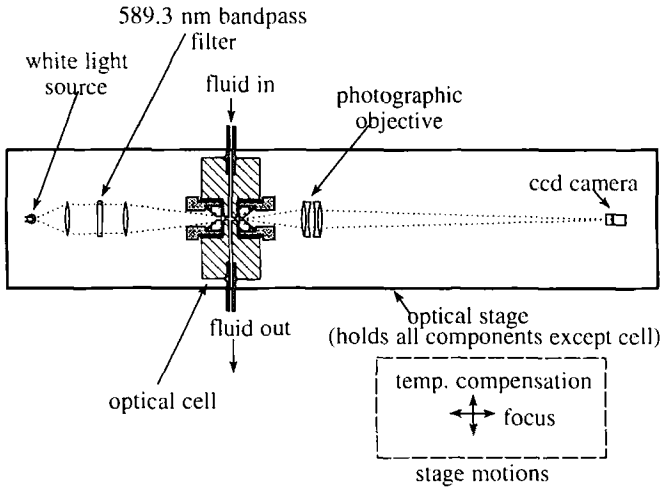

Fig. 3. Schematic of the optical system for refractive-index measurement. All components except cell are mounted to the optical stage.

length, f/1.4 photographic objective is used to image the cell onto a black-and-white CCD camera (Cohu Model 4810). The nominal magnification of the system is $10\times$, such that the image of the 1.0-mm face of the diamond window almost fills the CCD. If more magnification is desired, a $2.5\times$ microscope objective is placed between the lens and the camera. The optics are mounted on a stage which may be translated relative to the cell, in any of three perpendicular directions. The vertical and one of the horizontal adjustments are used to compensate for thermal expansion of the cell during temperature cycling. The other horizontal motion of the stage is used to focus the optical system alternately on the inside faces of the two diamond windows. This stage motion is accomplished by an Oriel Encoder Mike, driven by a Model 18010 controller. The micrometer has a range of 1.0 cm, with a readout precision of 0.1 μm. Figure 4 shows how the refractive index of the fluid in the cell is measured. The stage is first focused on the back window (inside surface), then translated to focus on the front window, and the distance is noted. This distance, divided into the actual distance between the windows (inside surfaces), is the refractive index of the fluid.

The main error associated with the determination of the refractive index is the subjectivity of the focusing on the two optical windows. Usually the focus is determined by examining the images of small specks of dirt or corrosion products that are adhering to the window. Repeated observations under constant conditions have shown that the optical thickness can be determined to about $\pm 10\,\mu$m (1 standard deviation). This

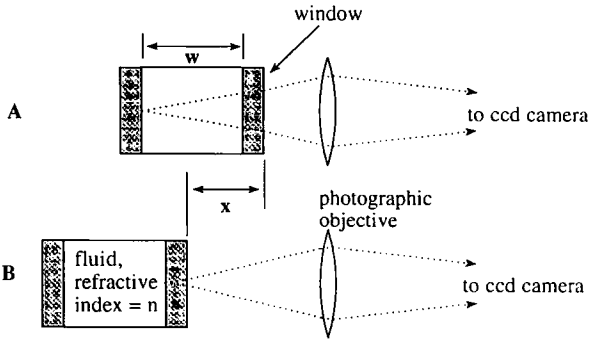

A: camera focused on back window

B: cell moved a distance x, such that camera is focused on front window

$n = w/x$

Fig. 4. Illustration of the technique for refractive-index measurement. The optical system is alternately focused on (inside) the back and front window surfaces.

corresponds to a typical uncertainty of $\pm 0.25\%$ in the refractive index. The uncertainty in density determination depends strongly on the density due to the nonlinearity of the Lorentz–Lorenz equation, Eq. (1). The uncertainty in density for pure water, based on a refractive index uncertainty of $\pm 0.25\%$, is given for various densities in Table I. Similar results are obtained for electrolyte solutions.

Obviously, the precision of the refractive index must be much better than the desired precision in the density, and the problem becomes more severe as the solution density goes down. However, the results here do not represent the limits of the technique. Greater precision in the determination

Table I. Uncertainty in Density Determination of Water Due to Uncertainty of $\pm 0.25\%$ in the Refracive-Index Determination

Density ($kg \cdot m^{-3}$)	Density uncertainty (%)
317	± 2.7
620	± 1.42
906	± 0.99

of refractive index could be achieved by engraving the diamond window surfaces. This would more precisely locate the surfaces, and would make it possible to use the electronic images of the surfaces to determine focus, greatly reducing the subjectivity of this step in the procedure. Alternatively, laser interferometry could be used to treasure the window separation, eliminating the need to determine focus altogether.

4. RESULTS

4.1. Water

A series of measurements of the refractive index of water as a function of temperature and pressure was made to test the validity of the assumption of constant specific refraction, by comparing measured densities to accurate values calculated from the Haar, Gallagher, and Kell (HGK) [3] equation of state. These measurements also eliminated certain experimental difficulties in the refractive-index measurement. First, the distance between the windows, w, is difficult to measure directly and changes with temperature due to thermal expansion. Second, due to spherical aberration introduced by the diamond windows and the fluid itself, the images of the windows are not absolutely sharp, and the position of "best" focus is somewhat subjective. Thus, measurements of refractive index using measured values of w may be offset from the true values and will differ for different observers. As a result, values of the specific refraction of water calculated

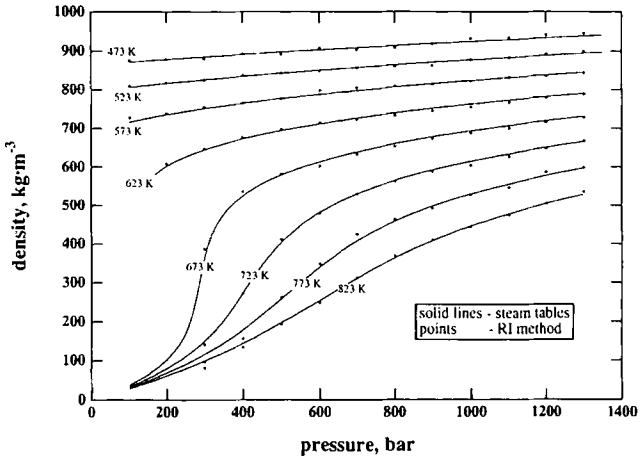

Fig. 5. team density vs pressure measurements, from 473 to 823 K. Data points were measured by the RI technique. Solid curves were calculated from the HGK equation of state [3].

from these values of refractive index would also be in question. To solve these difficulties, the *a priori* assumption of *constant* specific refraction was made. Then the data for water at a given temperature were made to give the best fit (in the least-squares sense) to the density data for water from the HGK equation of state, by the selection of an "effective" window separation, w_{eff}. The values of w_{eff} were then fitted as a linear function of temperature, in order to account for the variation of cell thickness due to thermal expansion. Then the fitted values of w_{eff} were used to recalculate

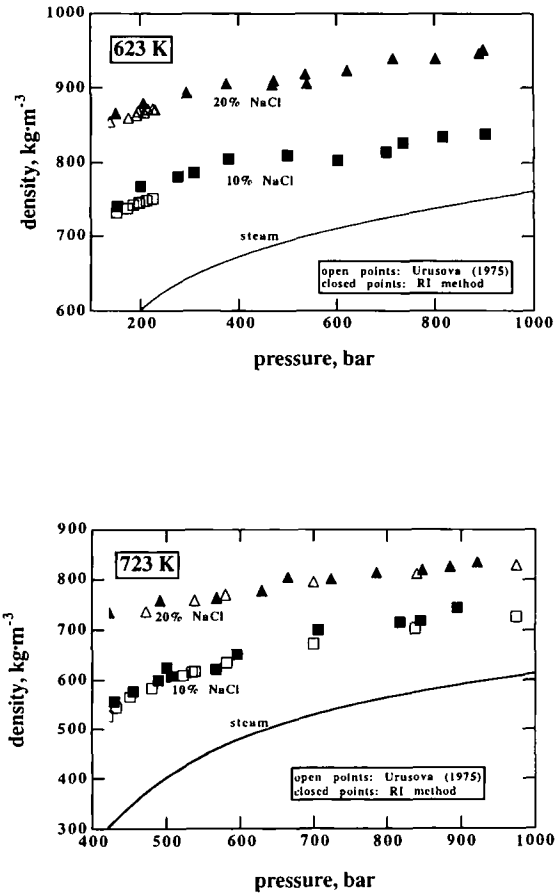

Fig. 6. Density vs pressure of NaCl solutions at 623 K (top) and 723 K (bottom). Solid points were measured by the RI technique, while open points are from the data of Urusova [5], measured by conventional techniques. Steam density is also shown for reference.

the density (still assuming constant specific refraction) as a function of pressure for each temperature. The resulting curves for temperatures between 473 and 823 K are shown in Fig. 5. The excellent agreement between the densities determined by the refractive index (RI) technique and the values from the HGK equation of state may be considered as proof-of-principle for the technique, at least for water. That is, if the specific refraction were not virtually independent of temperature and density, the two sets of data in Fig. 5 would not have agreed over such a wide range of variables. The choice of the appropriate value of the specific refraction is discussed in Section 5.

4.2. NaCl/Water Solutions

Sodium chloride is one of few salts for which extensive solution density data have been published at temperatures above 573 K. The NaCl/water system thus serves as a good test of the RI technique for measuring density in hydrothermal solutions. The specific refraction of NaCl solutions was determined from refractive index and density data [4] taken at room temperature, and it was assumed that the same value of refraction applies under hydrothermal conditions. Figure 6 shows plots of the density vs pressure data of Urusova [5] for 10 and 20 wt% NaCl solutions at 623 and 723 K, along with data under the same conditions using the RI technique. The agreement between the two sets of data is within the combined

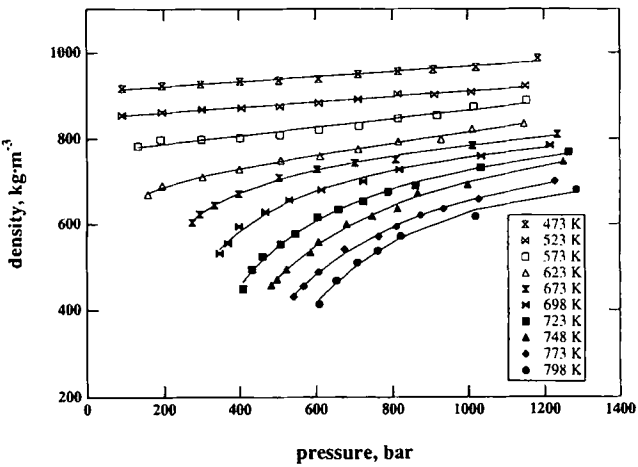

Fig. 7. Density vs. pressure for 1.0 molal $NaNO_3$ solutions, from 473 to 798 K. The left-hand terminus of each curve is the approximate locus of the liquid–vapor phase boundary.

uncertainties. Thus, deviations from constant specific refraction appear to be small or nonexistent, and the RI technique is shown to be valid even for fairly concentrated electrolyte solutions.

4.3. $NaNO_3$/Water Solutions

Having shown that the RI technique is effective for electrolyte solutions, an extensive study was undertaken of the $NaNO_3$/water system, for which no density data have been previously published at high temperatures. Figure 7 shows density vs pressure isotherms for a 1.0 molal solution, for temperatures from 473 to 798 K, in 50 K increments up to 673 K and 25 K increments thereafter. Each isotherm terminates at the liquid–vapor phase boundary, which was directly observed in the optical cell as the pressure was lowered. Figure 8 gives the analogous results for 0.25 molal $NaNO_3$ in water, from 673 to 798 K in 25 K increments.

By taking derivatives of the smoothed density profiles with respect to temperature and pressure, the thermal-expansion coefficient and isothermal compressibility may be determined, as shown for the 1.0 molal solution in Figs. 9 and 10, respectively. The critical temperature of the 1.0 molal solution, based on observations of the L–V phase boundary, was near 723 K. The apparent divergence of the compressibility in this region is further evidence for critical behavior. The variation in liquid–vapor critical temperature with $NaNO_3$ concentration is evident from Figs. 7 and 8; the

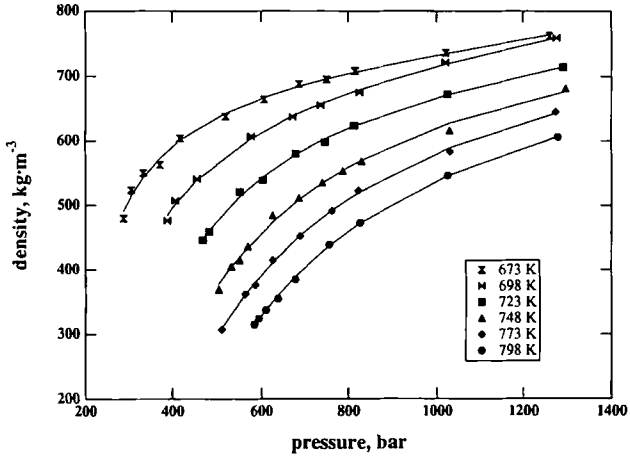

Fig. 8. Density vs pressure for 0.25 molal $NaNO_3$ solutions, from 673 to 798 K. The left-hand terminus of each curve is the approximate locus of the liquid–vapor phase boundary.

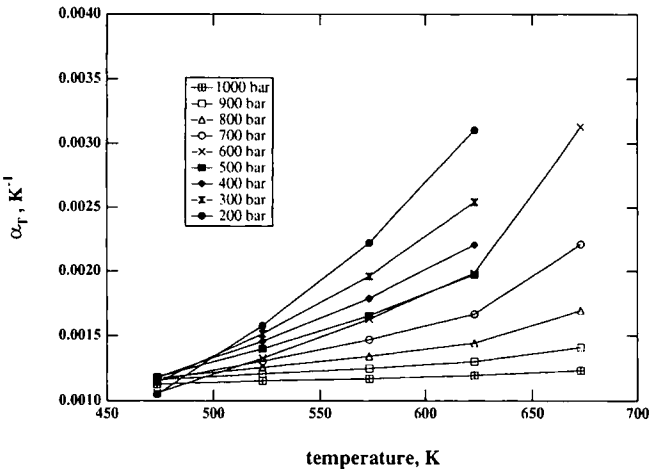

Fig. 9. Volume coefficient of thermal expansion vs temperature for 1.0 molal $NaNO_3$ solutions, for pressures between 200 and 1000 bar, determined by numerical differentiation of the data in Fig. 7.

steepest slopes (highest compressibility) in the ρ–p plots occur near 673 K for 0.25 molal solutions and near 723 K for 1.0 molal solutions. The RI technique is perhaps not the best method for density measurement near critical points, however, since fluids tend to be unstable there due to unavoidable temperature gradients.

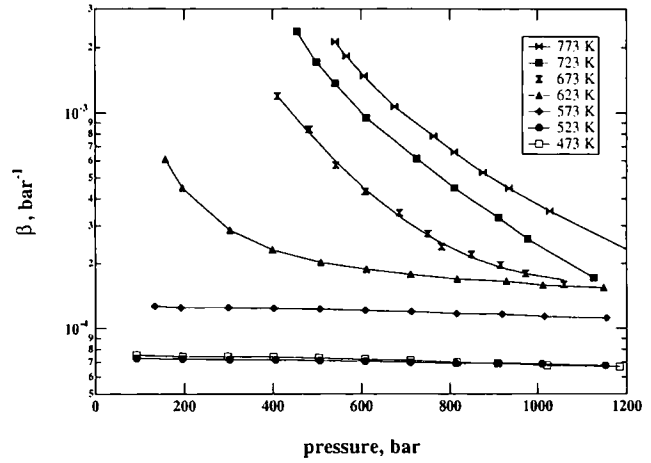

Fig. 10. Isothermal compressibility vs pressure for 1.0 molal $NaNO_3$ solutions, from 473 to 773 K, determined by numerical differentiation of the data in Fig. 7.

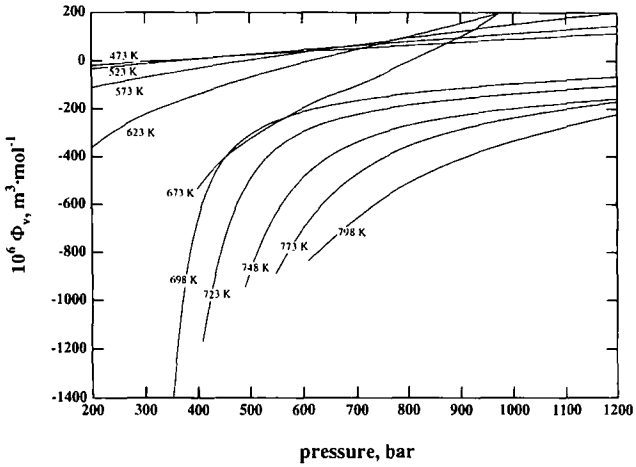

Fig. 11. Apparent molal volume of $NaNO_3$ in a 1.0 molal NaNO3/water solution vs pressure, from 473 to 798 K, determined from the fitted density profiles in Fig. 7.

As another example of the type of information that may be derived from ρ–p–T data, Fig. 11 shows the apparent molal volume Φ_v of the $NaNO_3$ in a 1.0 molal solution. The apparent molal volume is defined by

$$\frac{1 + m_2 M_2}{\rho_{soln}} = \frac{1}{\rho_w} + m_2 \Phi_v \tag{4}$$

Φ_v = apparent molal volume of the solute, $m^3 \cdot mol^{-1}$

M_2 = molecular weight of the solute, $kg \cdot mol^{-1}$

ρ_{soln} = mass density of the solution, $kg \cdot mol^{-3}$

ρ_w = density of pure water at the same temperature and pressure, $kg \cdot m^{-3}$

m_2 = molality of the solute, $mol \cdot kg^{-1}$

The apparent molal volume is an effective volume occupied by solute molecules, if one assumed that the water occupies the same volume it would in pure steam. Negative values of Φ_v are a consequence of the strong attraction between solvent and solute. The divergence of the apparent molal volume near 700 K and 400 bar is characteristic of a solution near its critical point (see, e.g., Ref. 6).

5. DISCUSSION

5.1. Relating Refractive Index to Density in Water

In Sections 2 and 4.1 we argue that the specific refraction of water may be taken as being independent of density and temperature when using the Lorentz–Lorenz equation to compute the density from the index of refraction. Now we attempt to justify this assumption. There is a wealth of refractive-index data in the literature for ice, water, and steam, as summarized by Schiebener et al. [7]. The data unfortunately do not extend to hydrothermal conditions, where the temperature and density are simultaneously large. However, the variation of specific refraction with density and temperature is very small in the regions where data exist. For example, the specific refraction of liquid water from 0 to 60°C changes from 0.2062 to 0.2059 $cm^3 \cdot g^{-1}$, according to the extremely accurate data of Tilton and Taylor [8]. The specific refraction of steam at 225°C over the density range 1–12 $kg \cdot m^{-3}$ varies from 0.2099 to 0.2096 $cm^3 \cdot g^{-1}$, according to the data of Achterman and Rögener [9]. In both of the previous examples, the refractive index was measured relative to air, at a wavelength of 0.589 μm. Schiebener et al. [7] fitted these and all other available high-quality data as a function of density, temperature, and wavelength, arriving at a 10-parameter fit. The authors state, "We do expect, but cannot substantiate with data, that the formulation will give good estimates of refractive index at temperatures much higher than given in Ref. 9, and that it will extrapolate correctly even into the supercritical regime." For illustrative purposes, we use their formulation to predict the specific refraction, R, at two sets of supercritical conditions (see Table II). We choose conditions which differ substantially in temperature and density so as to estimate the "worst-case" variations which might be expected in the specific refraction.

In the cell calibration procedure discussed in Section 4.1, a value of 0.206 $cm^3 \cdot g^{-1}$ was originally chosen for the specific refraction of water. This was based on the Tilton and Taylor [8] data and the assumption that water under hydrothermal conditions would be liquid-like insofar as the refractive index is concerned. The Schiebener formula is probably more accurate but it gives results that are essentially the same as ours, within

Table II. Specific Refraction, R, Under Two Sets of Supercritical Conditions

Temperature (°C)	Pressure (bar)	Density ($kg \cdot m^{-3}$)	R ($cm^3 \cdot g^{-1}$)
450	1000	613.8	0.2075
550	500	195.6	0.2077

experimental error, over the entire range of temperature and density that we studied.

The measurements described in this report are not absolute, in that we had to *assume* constant specific refraction in order to calibrate the system. Also, our experimental uncertainty of $\pm 0.25\%$ in the refractive index prevents us from observing variations in specific refraction as small as predicted by the Schiebener formulation. We merely state that our results show that the remarkably weak dependence of specific refraction on temperature and density extends into the supercritical regime, thus demonstrating that the RI technique is a valuable tool for density determination there. An absolute refractive index measuring technique, with an order of magnitude better precision, would be required in order to explore further the variability of the specific refraction in the supercritical regime.

5.2. Relating Refractive Index to Density in Electrolyte Solutions

For electrolyte solutions in water, the assumptions that go into the Lorentz–Lorenz equation are more suspect than for pure water. For example, Eq. (3) states that the specific refraction of a solution of sodium chloride in water can be predicted from a knowledge of the refractive indices and densities of crystalline sodium chloride and pure water. However, the environment of sodium and chloride ions in solution is very different from that in the crystal. Ions (particularly cations) polarize and bind to neighboring water molecules, and it is not unreasonable to assume that the polarizabilities of solvent and solute molecules are shifted relative to the pure substances. Experimentally, this has been found to be the case, as first noted by Fajans [10] and later elaborated by Bottcher [11]. For example, Fig. 12 shows the specific refraction vs mole fraction for sodium chloride solutions at 293 K, as measured and as predicted by Eq. (3). The relative difference, $\Delta R/R$, between measured and calculated specific refractions for the alkali chlorides at 293 K is shown in Fig. 13. The largest discrepancy is found for the smallest (therefore most highly polarizing) cation, Li^+, as might be expected. The discrepancies would not be troublesome if they could be captured by a more comprehensive theory, one that allows a prediction of specific refractivity as a function of temperature, pressure, and composition of a solution. The first step in that direction was taken by Bottcher [11], who postulated that the basic form of Eq. (3) is correct but that a more complicated function of refractive index [compared to $(n^2-1)/(n^2+2)$] is required. The "corrected" form of the L-L equation was able to account for the concentration dependence of the specific refractivity for a number of salts, at room temperature and atmospheric pressure. Leyendekkers and Hunter [12, 13] took a further step by including the

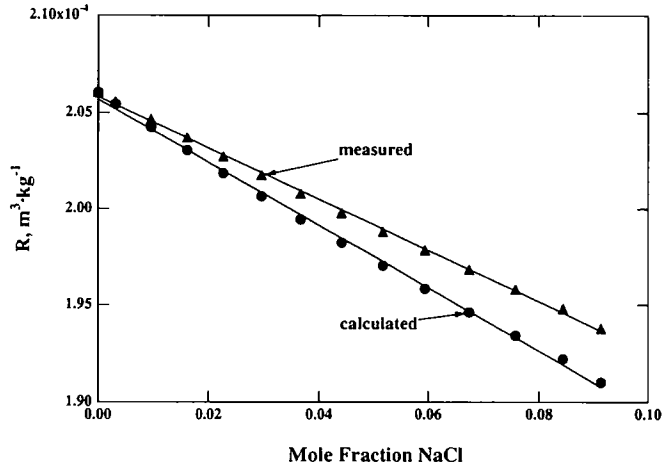

Fig. 12. Measured and calculated specific refraction vs mole fraction for NaCl solutions at 20°C. "Measured" values are derived from refractive index data in a standard handbook [4]. Calculated refraction was obtained from molar refraction data for water and crystalline NaCl.

effect of pressure as well as concentration. They used the Tamman–Tait–Gibson (TTG) model for the structure of electrolyte solutions and the formula of Eisenberg [14] for the water contribution to the refractive index, added a contribution due to the solute, and were able to fit the refractive index at 293 K as a function of composition and pressure, for a large number of electrolytes. They were not able to model the effect of temperature on the solute contribution to the refractive index, due to a lack of data in the literature. Since the structures of the hydration spheres around ions are presumed to cause the refractive-index discrepancies, and since these structures must change with temperature, no simple means exists at present to predict how the specific refraction of a solution varies with temperature. In the absence of theoretical or experimental guidance for the high-temperature behavior of binary systems, we make the simplest possible assumption; namely, that the specific refraction of both water and water/salt systems behaves similarly. A the level of precision of our technique, this is equivalent to assuming constant specific refraction. For water the value we choose is 0.206 $cm^3 \cdot g^{-1}$. For salt/water systems, we find the (easily measured) room-temperature value of the specific refraction and apply the same number at high temperatures, using the behavior of pure water (see Section 2) as a justification. We now need to consider whether the L-L equation for solutions handles the *composition* dependence of specific refraction. We note in Fig. 13 that the relative error in the concentration dependence of the specific refraction for NaCl solutions is small, not

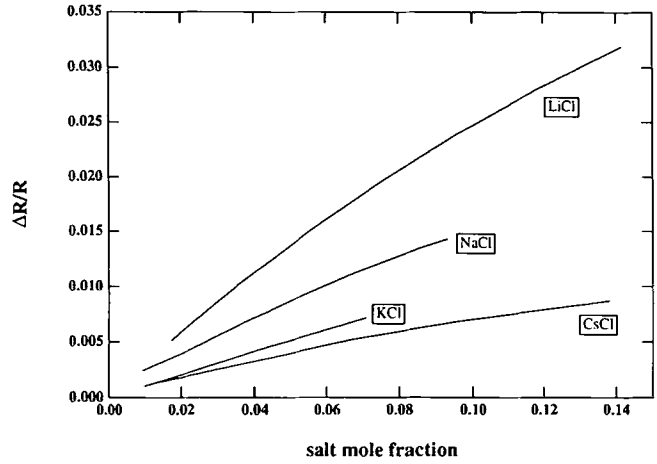

Fig. 13. Relative error $[=(R_{meas}-R_{calc})/R_{meas}]$ in the calculated specific refraction vs salt mole fraction, for the alkali chlorides in water at 20°C. "Measured" values are derived from refractive-index data in a standard handbook [4], and "calculated" values are derived from Eq. (3).

exceeding 2%, even for salt mole fractions as high as 0.10. One concludes that the L-L equation gives a very good approximation to the correct description of the relationship of refractive index to the density and composition of solutions. The approximation may be made even better by incorporating the observed variations of specific refraction with composition; that is, use the *measured* specific refraction (at room temperature) for solutions rather than the value calculated from Eq. (3). The ultimate justification for using the L-L equation to measure densities in hydrothermal solutions must lie in the comparison with other techniques for density determination under the same conditions. As we showed in Section 4, at least for the NaCl/water system, the RI technique using the L-L equation works well.

The near-independence of specific refraction on temperature and density is sensible when considered on an energetic basis. The refractive index is a measure primarily of the strength of the interaction of the electric field of the light wave with the electrons in the molecules comprising the fluid. Most of the electrons in a typical molecule are not involved in chemical bonding, so their orbitals differ only slightly from the atomic orbitals of the atoms comprising the molecule. For those electrons involved in bonding, the bond stabilization energies are small compared to the binding energies (ionization potentials) of the electrons in the separated atoms. Finally, the interactions between molecules in a dense fluid give rise to interaction

energies that are more than an order of magnitude smaller than the bond stabilization energies. Typical values are given as follows ionization potential, 1500 $kJ \cdot mol^{-1}$; bond energy, 400 $Kj \cdot mol^{-1}$; and hydrogen bond, 6–12 $Kj \cdot mol^{-1}$. One should therefore expect that the polarizability of a fluid should arise mainly from the atomic polarizabilities of the constituents, to be modified somewhat by the chemical bonds, and to be hardly affected by the interactions between molecules. This is precisely in accord with experimental observations, as pointed out by Born and Wolf [15]. The refractive index, which arises from the polarizability, thus has the virtue of being an easily measured quantity that has a simple relationship to density but is almost insensitive to other variables for a fluid of a given composition. More refined treatments [11–13], which include the effects of solvent structure and solvent-solute interactions on the refractive index, are available but are not needed if one is content with density accuracy on the order of a few percent. The method of measuring refractive index used in this work limits the imprecision of the density to the order of ± 1–3% at best; interferometric techniques for refractive index measurement could dramatically reduce the experimental error and possibly allow the observation of the more subtle effects mentioned above.

6. CONCLUSIONS

A new technique has been developed for measuring the density of hydrothermal systems, through the relationship between density and refractive index. The technique is shown to be valid by comparison to data taken using conventional techniques, for pure water and the water/NaCl systems. New data are reported for the density, thermal expansivity, compressibility, and apparent molal volume of the $NaNO_3$/water system.

ACKNOWLEDGMENTS

The author is grateful to his colleague David Schiferl for many useful suggestions about the design and operation of high-temperature, high-pressure optical cells. This work was sponsored by the Westinghouse Hanford Corporation under the auspices of the DOE.

REFERENCES

1. H. A. Lorentz, *Ann. Phys.* **9**:641 (1880).
2. L. V. Lorenz, *Ann Phys.* **11**:70 (1880).
3. From the program STEAM, J. S. Gallagher and L. Haar, NBS Standard Reference Database 10 (U.S. National Bureau of Standards, 1985).

4. *Handbook of Chemistry and Physics*, 50th ed. (Chemical Rubber Company, Cleveland, OH, 1969), p. D-202.
5. M. A. Urusova, *Russ. J. Inorg. Chem.* **20**:1717 (1975).
6. J. M. H. Levelt Sengers, C. M. Everhart, G. Morrison, and K. S. Pitzer, *Chem. Eng. Comm.* **47**:315 (1986).
7. P. Schiebener, J. Straub, J. M. H. Levelt Sengers, and J. S. Gallagher, *J. Phys. Chem. Ref. Data* **19**:677 (1990).
8. L. W. Tilton and J. K. Taylor, *J. Res. Natl. Bur. Stand.* **20**: 419 (1938).
9. H.-J. Achtermann and H. Rögener, in *Proc. 10th Int. Conf. Prop. Steam*, V. V. Sytchev and A. A. Alexandrov, eds. (MIR, Moscow, 1986), Vol. 2, p. 29.
10. K. Fajans, *Z. Elektrochem.* **34**:502 (1928).
11. C. J. F. Bottcher, *Rec. Trav. Chim.* **65**:39 (1946).
12. J. V. Leyendekkers and R. J. Hunter, *J. Phys. Chem.* **81**:1657 (1977).
13. J. V. Leyendekkers and R. J. Hunter, *J. Chem. Eng. Data* **22**:427 (1977).
14. H. Eisenberg, *J. Chem. Phys.* **43**:3887 (1965).
15. M. Born and E. Wolf, *Principles of Optics*, 5th ed. (Pergamon Press, Oxford, 1975), pp. 88–90.